



Paleoceanography and Paleoclimatology

Supporting Information for

Oxygenation of offshore Southern California Marine Basins through the Holocene

Hannah M. Palmer^{1,2}, Tessa M. Hill^{1,2}, Esther G. Kennedy^{1,2}, Peter Roopnarine³, Sonali Langlois⁴, Katherine R. Reyes⁵, and Lowell Stott⁶

1. Earth and Planetary Sciences, University of California, Davis
2. Bodega Marine Laboratory, University of California, Davis
3. California Academy of Sciences
4. Santa Rosa Junior College
5. Dominican University of California
6. University of Southern California

Contents of this file

Figures S1 to S5
Tables S1 to S2

Introduction

Supporting information contains five supporting figures and two supporting tables. All methodology is discussed in main text.

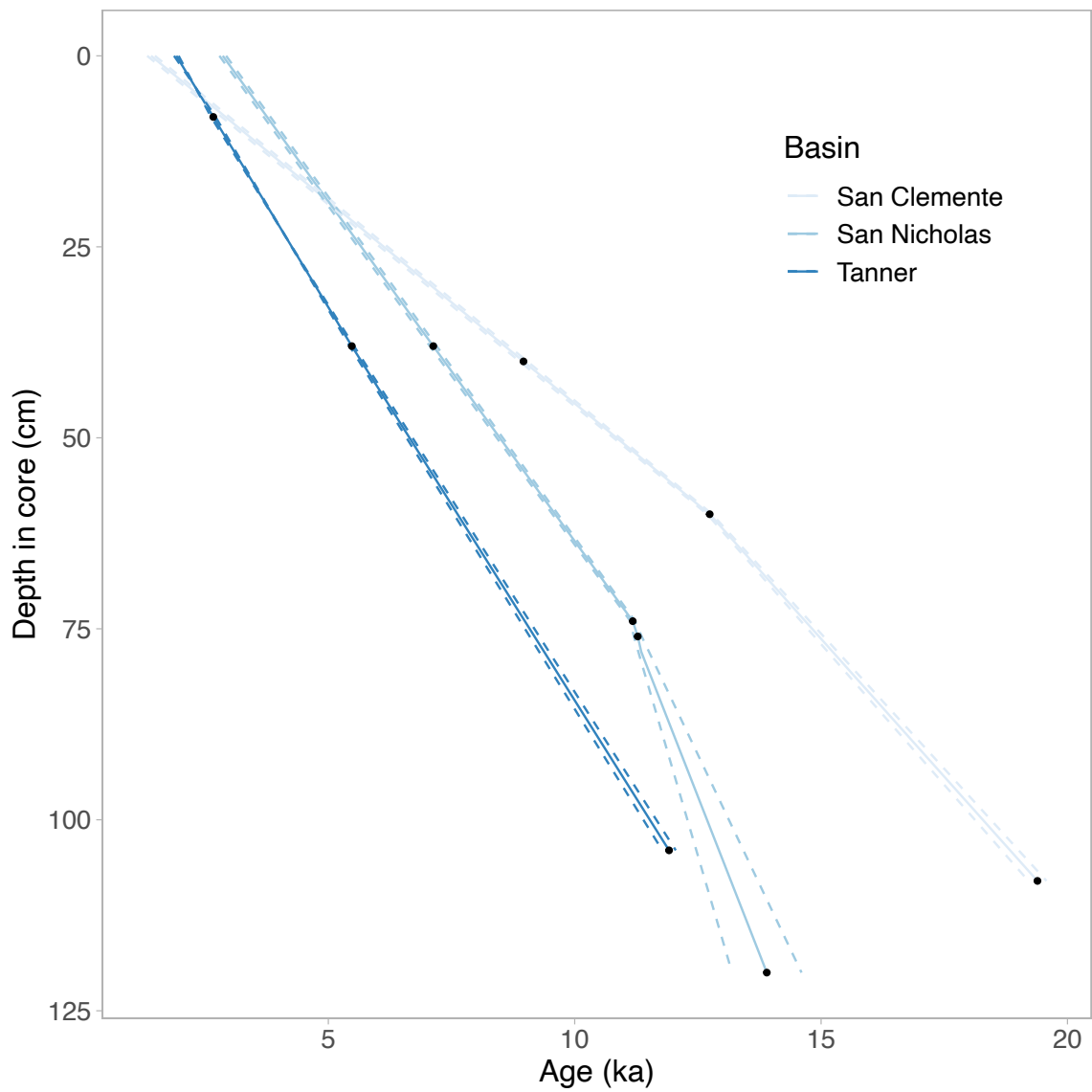


Figure S1. Radiocarbon-based age model for three cores included in study. Age shown in thousands of years before present. Linear interpolation (solid lines, Tanner= dark blue, San Nicolas = medium blue, San Clemente = light blue) between radiocarbon dates (black dots). Dashed lined represent +/- 1 sigma years.

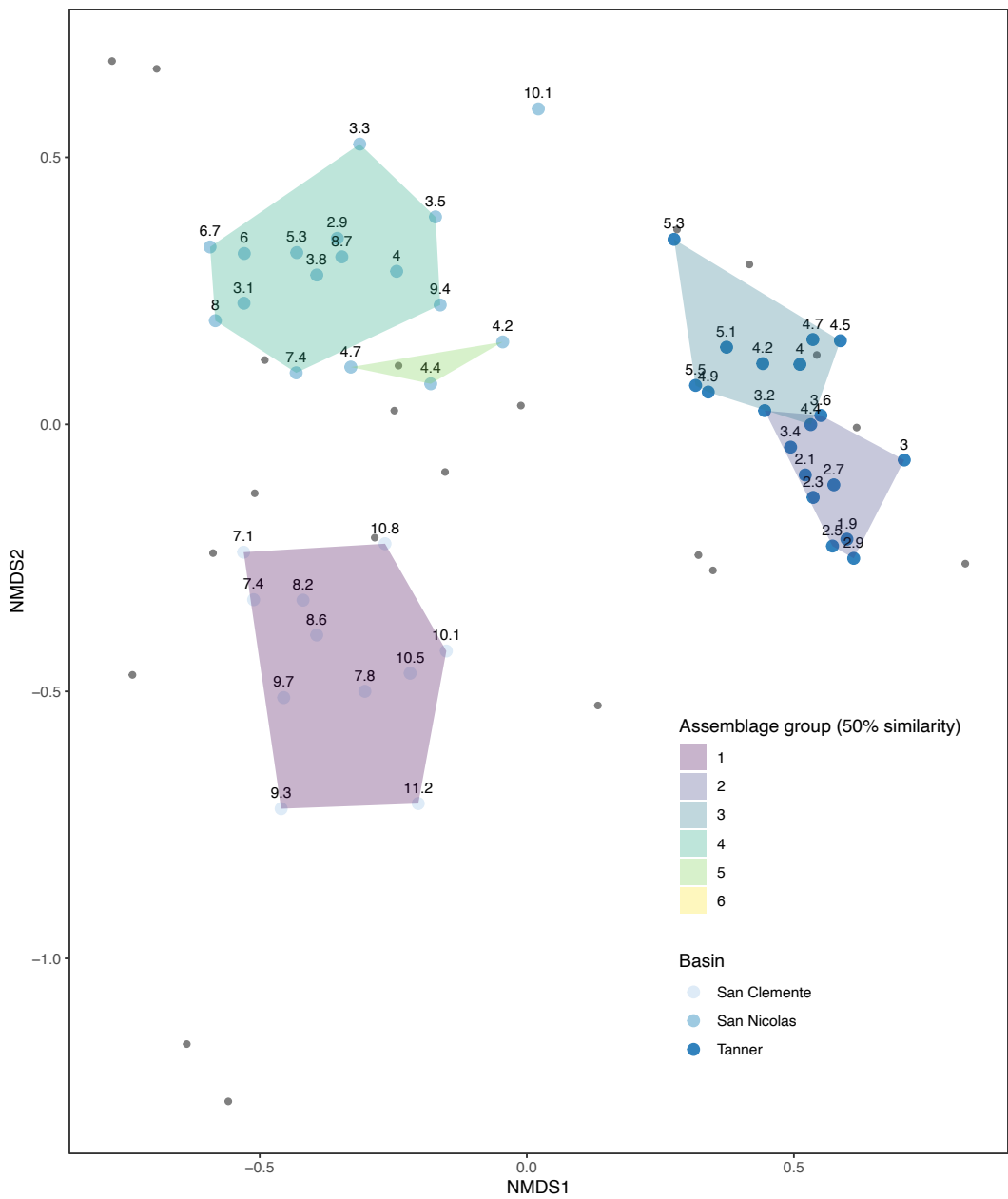


Figure S2. Non-metric multidimensional scaling plot of all benthic foraminiferal assemblages through time from three cores. Species are plotted as small gray dots. All other points represent assemblages at each interval through time at each of the three cores. Label is age in thousands of years before present. Colored dots represent each basin: Tanner= dark blue, San Nicolas = medium blue, San Clemente=light blue. Clusters show assemblages with 50% similarity, calculated using cluster analysis; five clusters are represented.

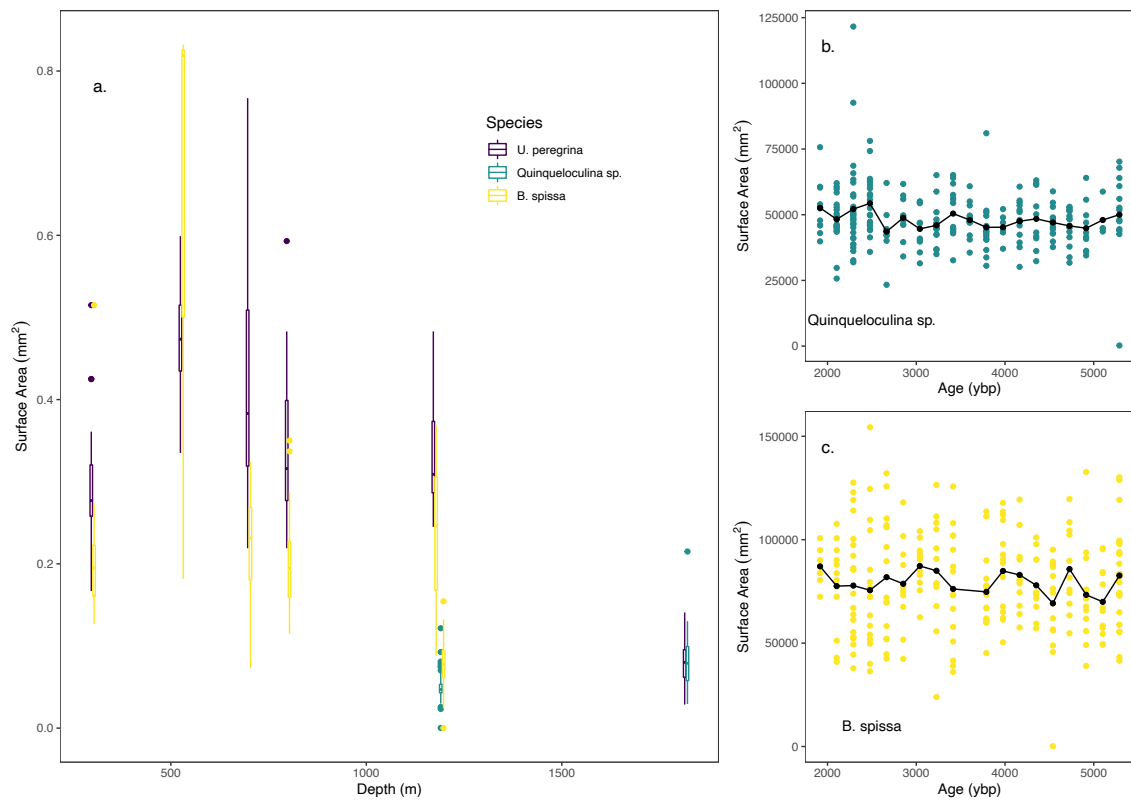


Figure S3. Shell surface area (mm^2) vs. water depth (m) at all points in time (a.). Data shown here indicate all points in time from each water depth. Colors represent species: U. peregrina = purple, Quinqueloculina sp. = green, B. spissa = yellow. Surface area of Quinqueloculina sp. (b.) and B. spissa (c.) vs. time in years before present from Tanner Basin.

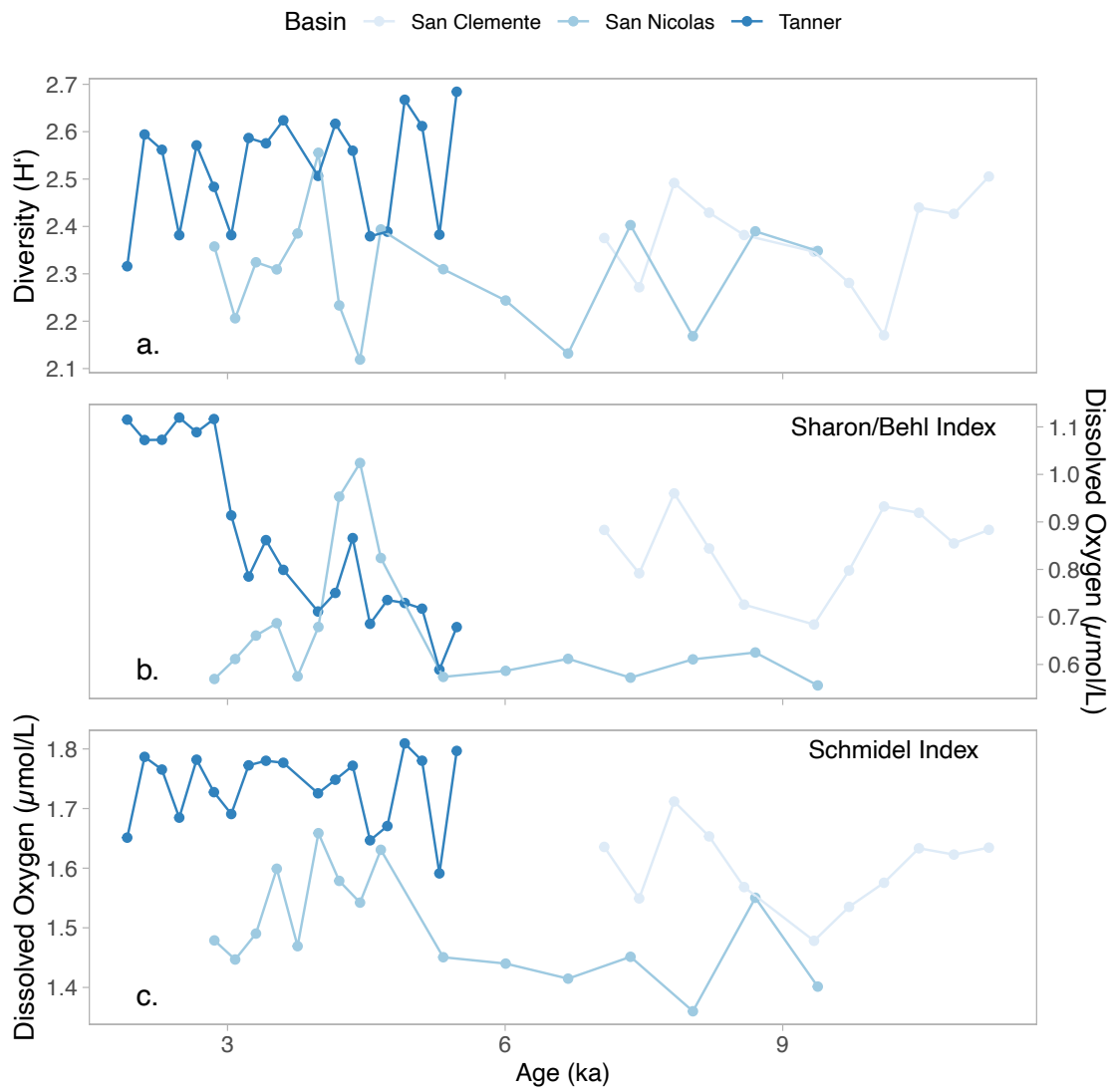


Figure S4. Diversity (Shannon Index, a.), reconstructed dissolved oxygen concentration using Sharon-Behl Index (b.), reconstructed dissolved oxygen concentration using Schmidel Index (c.) for three cores (Tanner= dark blue, San Nicolas = medium blue, San Clemente = light blue) vs. age in thousands of years before present.

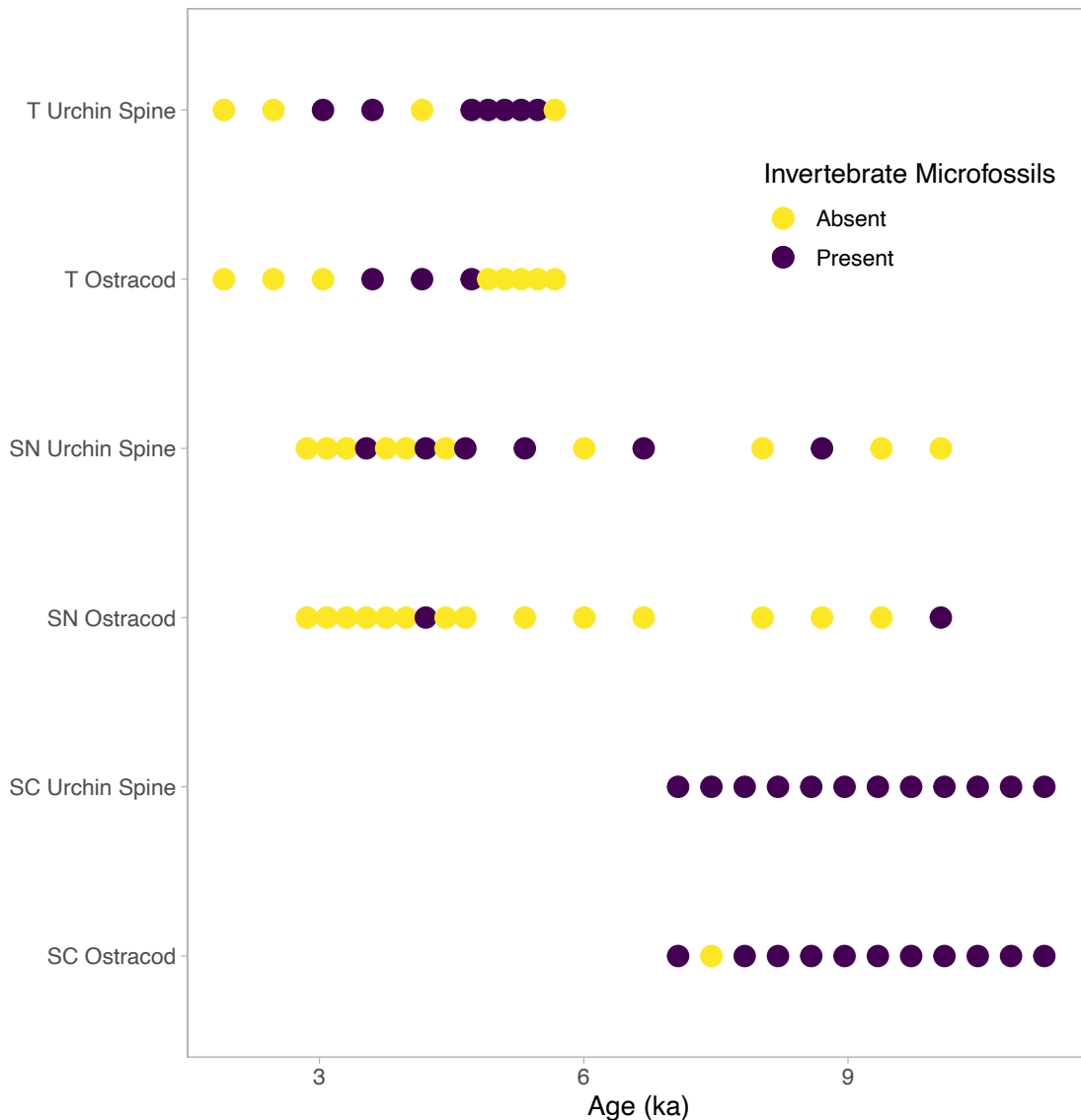


Figure S5: Presence and absence of metazoan microfossils (urchin spines and ostracods) through time (age in thousands of years before present) for each basin (Tanner (T), San Nicolas (SN), and San Clemente (SC)). Presence is purple, absence is yellow.

Basin	Core	Sample Interval	Source	Age (¹⁴C years)	±	1σ minimum calendar age	1σ maximum calendar age	Age (years before present)	Sed rate (cm kyr⁻¹)
Tanner	EW95 04-09	8-10 cm	Stott et al., 2000	1950	50	2619	2712	2666	10.67
Tanner	EW95 04-09	38- 40 cm	This paper	5290	30	5433	5521	5477	10.25
Tanner	EW95 05-09	104-106 cm	Stott et al., 2000	10790	60	11778	12051	11915	
San Nicolas	EW95 04-08	38-40 cm	Stott et al., 2000	6780	50	7062	7198	7130	8.89
San Nicolas	EW95 04-08	74-76 cm	This paper	10330	35	11130	11225	11178	16.48
San Nicolas	EW95 04-08	76-78 cm	Stott et al., 2000	10460	70	11200	11359	11280	16.48
San Nicolas	EW95 04-08	120-122 cm	Stott et al., 2000	12870	160	13193	14603	13898	
San Clemente	EW95 04-08	40-42 cm	Stott et al., 2000	8550	60	8882	9039	8960	5.29
San Clemente	EW95 04-08	60-62 cm	This paper	11430	40	12690	12789	12739	7.21
San Clemente	EW95 04-08	108-110 cm	Stott et al., 2000	16650	50	19575	19207	19391	

Table S1. Radiocarbon ages and age model for all three cores examined here.

Species	Oxygen Classification	Modified from Sharon-Behl	Citation for oxygenation affinity
<i>Bolivina argentea</i>	Suboxic		Sharon et al., 2021
<i>Bolivina pseudoberyethes</i>	Dysoxic		Sharon et al., 2021
<i>Bolivina spissa</i>	Suboxic		Sharon et al., 2021
<i>Bulimina tenuata</i>	Dysoxic		Sharon et al., 2021
<i>Cassidulina</i> sp.	Suboxic		Sharon et al., 2021
<i>Chlistomella ovoidea</i>	Suboxic		Sharon et al., 2021
<i>Cibicides mckannai</i>	Weakly hypoxic to oxic	Modified	Kaiho 1994
<i>Cibicides</i> sp.	Weakly hypoxic to oxic	Modified	Kaiho 1994
<i>Elphidium</i> sp.	Weakly hypoxic to oxic		Sharon et al., 2021
<i>Epistominella exigua</i>	Suboxic		Sharon et al., 2021
<i>Epistominella pacifica</i>	Weakly hypoxic to oxic	Modified	Cannarito and Kennett 1999
<i>Furstenkoina</i> sp.	Suboxic	Modified	Kaiho 1994
<i>Globobulimina barbata</i>	Suboxic	Modified	Ohkushi et al., 2013
<i>Globobulimina ovata1</i>	Suboxic	Modified	Ohkushi et al., 2013
<i>Globobulimina ovata2</i>	Suboxic	Modified	Ohkushi et al., 2013
<i>Globobulimina pacifica</i>	Suboxic	Modified	Ohkushi et al., 2013
<i>Globocassidulina</i> sp.	Suboxic		Sharon et al., 2021
<i>Globocassidulina subglobosa</i>	Suboxic		Sharon et al., 2021
<i>Hansenisca soldanii</i>	Weakly hypoxic to oxic	Modified	De and Gupta 2010
<i>Hansenisca</i> sp.	Weakly hypoxic to oxic		Sharon et al., 2021
<i>Melonis affinis</i>	Suboxic	Modified	Kaiho 1994
<i>Nonionella stella</i>	Dysoxic		Sharon et al., 2021
<i>Oridorsalis umbonatus</i>	Suboxic		Sharon et al., 2021
Other			
<i>Pyrgo murrhina</i>	Weakly hypoxic to oxic		Sharon et al., 2021
<i>Quinqueloculina</i> sp.	Weakly hypoxic to oxic		Sharon et al., 2021
<i>Quinqueloculina</i> sp2.	Weakly hypoxic to oxic		Sharon et al., 2021
<i>Uvigerina peregrina</i>	Suboxic		Sharon et al., 2021
<i>Uvigerina proboscoidea</i>	Suboxic		Sharon et al., 2021
<i>Uvigerina</i> sp.	Suboxic		Sharon et al., 2021

Table S2. Oxygen affinity for all species examined here and utilized in oxygen transfer functions.